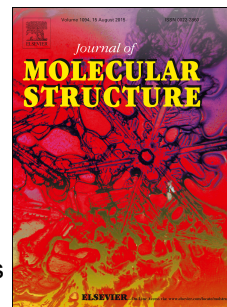


Journal Pre-proof

Synthesis and structural characterization of cocrystals of isoniazid and cinnamic acid derivatives

Syed Muddassir Ali Mashhadi, Dmitri Yufit, Huiyu Liu, Paul Hodgkinson, Uzma Yunus



PII: S0022-2860(20)30946-7

DOI: <https://doi.org/10.1016/j.molstruc.2020.128621>

Reference: MOLSTR 128621

To appear in: *Journal of Molecular Structure*

Received Date: 17 April 2020

Revised Date: 26 May 2020

Accepted Date: 4 June 2020

Please cite this article as: S.M.A. Mashhadi, D. Yufit, H. Liu, P. Hodgkinson, U. Yunus, Synthesis and structural characterization of cocrystals of isoniazid and cinnamic acid derivatives, *Journal of Molecular Structure* (2020), doi: <https://doi.org/10.1016/j.molstruc.2020.128621>.

This is a PDF file of an article that has undergone enhancements after acceptance, such as the addition of a cover page and metadata, and formatting for readability, but it is not yet the definitive version of record. This version will undergo additional copyediting, typesetting and review before it is published in its final form, but we are providing this version to give early visibility of the article. Please note that, during the production process, errors may be discovered which could affect the content, and all legal disclaimers that apply to the journal pertain.

© 2020 Published by Elsevier B.V.

Credit Author Statement

Synthesis and structural characterization of cocrystals of isoniazid and cinnamic acid derivatives

Syed Muddassir Ali Mashhadi: Conceptualization; Data curation; Formal analysis; Funding acquisition; Investigation; Methodology; Writing - original draft; Writing - review & editing

Dmitri Yufit: Data curation; Formal analysis; Software; Writing - review & editing

Huiyu Liu: Data curation; Formal analysis; Writing - review & editing

Paul Hodgkinson: Conceptualization; Data curation; Formal analysis; Methodology; Project administration; Resources; Software; Supervision; Validation; Visualization; Writing - review & editing

Uzma Yunus: Conceptualization; Formal analysis; Funding acquisition; Project administration; Resources; Supervision; Validation; Visualization; Writing - review & editing

Synthesis and structural characterization of cocrystals of isoniazid and cinnamic acid derivatives

Syed Muddassir Ali Mashhadi^{1,2*}, Dmitri Yufit², Huiyu Liu², Paul Hodgkinson^{2*}, Uzma Yunus¹

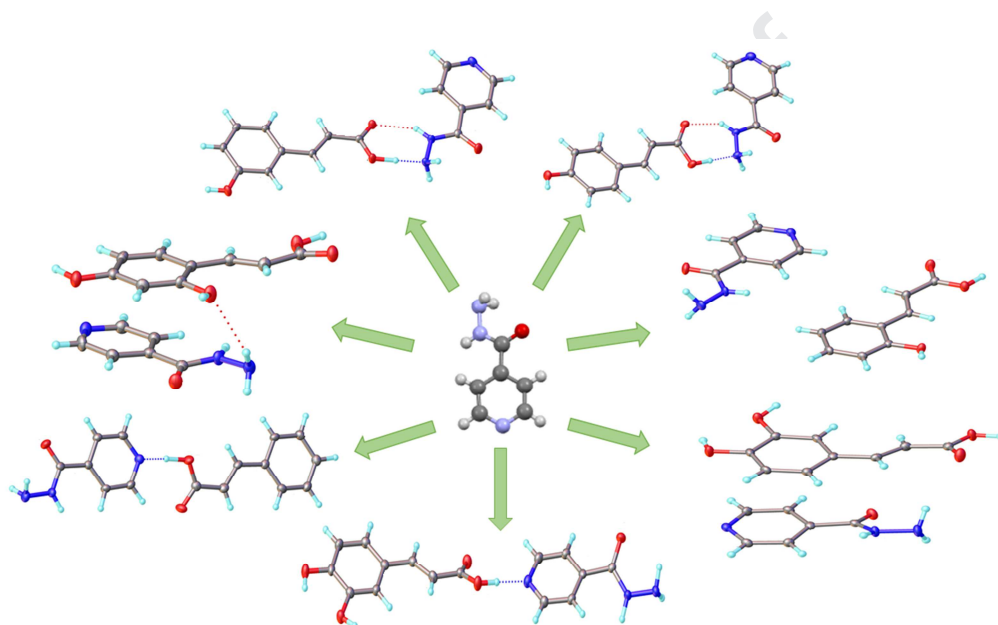
¹ Department of Chemistry, Allama Iqbal Open University, Islamabad, Pakistan

² Department of Chemistry, Durham University, Stockton Road, Durham DH1 3LE, United Kingdom

*muddassir_bakie@yahoo.com

*paul.hodgkinson@durham.ac.uk

* Corresponding author.



Abstract

Isoniazid is a key antitubercular agent which exhibits poor chemical stability in the solid state. Cocrystallization with hydroxyl derivatives of cinnamic acid, which themselves possess antitubercular and antioxidant activity, may produce solid forms with improved pharmaceutical properties. The complementary nature of the functional groups of isoniazid and the chosen coformers resulted in a high success rate for cocrystal formation. The three previously unknown cocrystal forms, plus a new polymorph were characterized by solid-state NMR, DSC, PXRD and single crystal XRD. Three previously known cocrystals were also synthesized and characterized. NMR chemical shifts were observed to distinguish between a key synthon involving the carboxylic acid of cinnamic acid.

Introduction

The World Health Organization (WHO) has declared tuberculosis (TB) to be a global emergency. Treatment of TB with a single drug in isolation, however, is associated with risks of drug resistance, and the International Union against TB and Lung Diseases has recommended the use of fixed-dose combinations (FDCs) of first line anti-TB drugs to prevent monotherapy and drug resistance.[1][2] Isoniazid (INH), a highly active drug recommended by WHO against *M. tuberculosis*, is being used as the primary constituent of different FDCs and “triple therapies” to combat tuberculosis since 1952.[3] Having good

solubility and stability[4] there are, however, concerns about the stability of FDCs involving INH and rifampicin (RIF), another antitubercular antibiotic; RIF exhibits significantly impaired bioavailability in FDC dosage forms when compared to formulations containing only RIF.[5] RIF and INH cross-reaction[6] in the solid formulation environment yields isonicotinyl hydrazone under acidic as well as basic conditions on storage of solid FDC formulations under accelerated stability test conditions.[7] Moisture absorbance by tablet INH and ethambutol was also observed under accelerated stability test conditions.[8] These interactions lead to decreased stability of the FDCs.

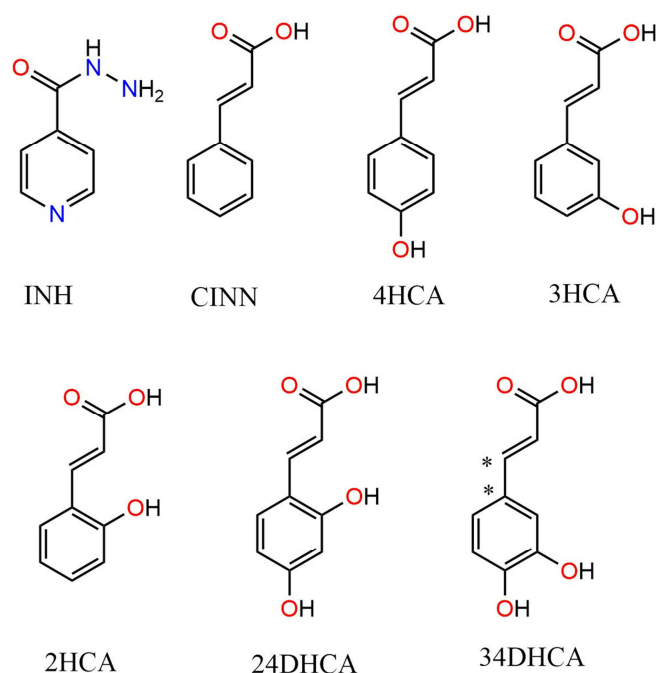
Oxidative stress is considered responsible for the hepatotoxicity in the TB patients when administered with anti-TB drugs like INH, RIF and pyrazinamide.[9] Treatment with antioxidants like curcumin, silymarin and *N*-acetyl cysteine have shown hepato-protective results.[9] This suggest a potential adjuvant role of antioxidant drugs[10] when combined with anti-TB treatments.[11] Oxidation reactions are also one of the main causes of degradation of Active pharmaceutical ingredients (APIs) or tablets. Hence cocrystallization with antioxidants may reduce oxidative stress in tuberculosis patients during treatment and may increase the shelf-life of FDCs.

Natural products bearing the cinnamoyl moiety have attracted much attention due to their broad spectrum of biological activities and low toxicity. Trans-cinnamic acid derivatives have shown to augment the activity of various antibiotics against *Mycobacterium avium*[12] and also show antioxidant, anti-inflammatory and cytotoxic properties.[13][14] Cinnamic acid derivatives bearing phenolic hydroxyl groups also have free radical scavenging properties[15][16], and so may sacrificially reduce the chemical degradation of easily oxidized APIs, such as INH. Weakly basic drugs show decreased solubility and dissolution as pH increases from 1 to 7 along the gastrointestinal tract, which is detrimental to drug absorption. Cocrystallization of basic drugs, such as INH, with acidic cofomers can mitigate these effects.[17] Moreover, the degradation of RIF and INH due to hydrazone formation in FDC may potentially be countered by masking the hydrazide group through cocrystallization, as well as allowing INH to be combined with an antioxidant in a single tablet. In this present study, hydroxyl derivatives of cinnamic acid were employed to synthesize new cocrystal forms of INH (Scheme 1).

Crystal engineering provides an opportunity to develop new solid forms based on non-covalent intermolecular forces interactions among components[18], and pharmaceutical cocrystallization[19],[20],[21],[22],[23] is being widely investigated as a strategy to improve the physicochemical and stability properties of solid dosage forms of APIs.[24],[25],[26] Formulation of two or more APIs having complementary functional groups into a single dosage can save manufacturing, packaging and storage resources as well as being provide convenient to patients. As an example, sildenafil-acetylsalicylic acid cocrystal has improved physiochemical properties with higher dissolution rates compared to the marketed form,of sildenafil citrate.[27] One approach to understand cocrystals structures is to identify sub structural units, commonly termed “supramolecular synthons”. [28] For example, the synthon formed between the N of pyridine and the hydroxyl of carboxylic acid has been previously used to design cocrystals of INH.[29],[30] Hydroxyl derivatives of cinnamic acid provide potentially additional opportunities for hydrogen bonding with INH.[31]

Solid-state NMR is frequently used to characterize cocrystals, particularly when they have been produced by mechanical grinding and so single-crystal diffraction is not possible.[32], [33],[34] NMR chemical shifts are sensitive to local chemical environments, and so, for example, can distinguish between cases where a hydrogen has been transferred between API

and coformer to generate a salt form. Moreover, advances in quantum chemistry mean that chemical shifts can now be calculated with good precision given a crystal structure, allowing correlations between structure and solid-state NMR shifts to be investigated, for example, on cinnamic acid and derivatives.[35]



Scheme 1: Chemical structures and abbreviated names used for molecules used in this study: isoniazid (INH), cinnamic acid (CINN), 2-hydroxycinnamic acid (2HCA), 3-hydroxycinnamic acid (3HCA), 4-hydroxycinnamic acid (4HCA), 2,4-dihydroxycinnamic acid (24HCA) and 3,4-dihydroxycinnamic acid (34DHCA). The 34DHCA molecule adopts the conformation shown in most of the structures obtained but adopts a conformation with a 180° rotation about the bond indicated with asterisks in one of the forms.

Experimental

Synthesis of Cocrystals

Isoniazid and coformers were purchased from Sigma-Aldrich and used without further purification. All samples analyzed were produced by crystallization. In the case of 4HCA, 3HCA and 2HCA coformers, crystalline samples of the cocrystals with INH were obtained directly by dissolving 1:1 molar ratio of coformer and INH separately in methanol. The solutions were mixed and heated at 55°C for 30 mins with stirring and left at room temperature. Slow evaporation led to the formation of colored crystals after some days, which were filtered out.

CINN, 24DHCA and 34DHCA failed to form cocrystals via this route, but crystalline samples were obtained by recrystallization of powder materials produced by liquid assisted grinding (it is plausible that microscopic crystals produced by grinding acted as seed crystals in the subsequent crystallization step). Except for INH-CINN, where a 2:1 mixture of ethanol/acetonitrile was used as the solvent, the raw grinding product was obtained by methanol-assisted grinding of a 1:1 stoichiometric ratio for 35 mins. Final crystalline products were then obtained by slow evaporation of the ground product using the same solvent used for liquid-assisted grinding. The product in the case of 34DHCA was not fully reproducible; recrystallization of the grinding material obtained after 35 mins generally produced a new co-

crystal polymorph (designated Form 4), while the recrystallization of the product after longer grinding (about 50 minutes) generally produced a mixture of forms, partly Form 4, but also some Form 1 (as identified by single-crystal XRD). This complex polymorphic behavior was not investigated further.

Differential Scanning Calorimetry (DSC)

Differential Scanning Calorimetry (DSC) experiments were performed on Perkin Elmer DSC 8500 running from 30 to 350 °C at 10 °C per minute in a standard aluminum pan in an inert atmosphere (helium). All the samples had decomposed by 350 °C and so only the first heating run is shown. The Pyris software (version 13) was used to remove baseline gradients before plotting and determination of transition temperatures.

Solid-State NMR Spectroscopy

Solid-state ^{13}C NMR spectra were obtained on a Bruker Avance III HD spectrometer using a ^{13}C resonance frequency of 125.7 MHz (magnetic field strength of 11.7 T). Approximately 100 mg of crystalline sample was packed into a zirconia 4 mm rotor with a Kel-F cap. The cross-polarization magic angle spinning (CP-MAS) pulse sequence was used for spectral acquisition at a spinning rate of 10.00 kHz, with the magic angle setting calibrated using KBr. Spectra were obtained using a recycle delay of 180 seconds and number of scans was 320 for cocrystals, while the corresponding parameters for INH were 600 seconds and 120 scans respectively. Data sets were Fourier transformed with a 5 Hz line broadening and phase corrected to produce a frequency domain spectrum. The chemical shifts were referenced indirectly to neat tetramethylsilane by setting the high frequency signal of adamantane to 38.5 ppm. ^1H NMR spectra were also obtained under fast MAS conditions. These exhibited some unusual features which will be explored in a separate publication; see the Supplementary Information (SI) figure S19.

X-Ray Crystallography

Powder X-ray diffraction measurements were performed on a Bruker D8 Advance diffractometer equipped with Cu $K\alpha_{1,2}$ source ($\lambda = 1.5418 \text{ \AA}$), Lynx-eye Soller PSD detector and variable slits. The samples produced by crystallization were lightly ground and sprinkled onto Si slides covered with a thin layer of Vaseline. Each PXRD pattern was collected at room temperature for 30 minutes over a 2θ range of 3–55° using a step size of 0.02°.

The X-ray single crystal data were collected at 120.0(2) K using Mo $K\alpha$ radiation ($\lambda = 0.71073 \text{ \AA}$) on Bruker D8Venture (Photon100 CMOS detector, $I\mu\text{S}$ -microsource, focusing mirrors) and Agilent XCalibur (structures INH-4HCA and INH-34DHCA Form 1; Sapphire-3 CCD detector, fine-focus sealed tube, graphite monochromator) diffractometers equipped with the Cryostream (Oxford Cryosystems) open-flow nitrogen cryostats. All structures were solved by direct method and refined by full-matrix least squares on F^2 for all data using Olex2[36] and SHELXTL[37] software. All non-disordered non-hydrogen atoms were refined anisotropically. Hydrogen atoms were refined isotropically, except for hydrogen atoms not involved in hydrogen bonding in structures INH-4HCA and INH-3HCA, which were placed in calculated positions and refined in riding mode. Crystal data and parameters of the refinements are listed in Table 2. Crystallographic data for the structures have been deposited with the Cambridge Crystallographic Data Centre as supplementary publications CCDC 1993881–1993887.

CASTEP Calculations

First principles calculations were carried out using the GIPAW method implemented in CASTEP[38], version 17.2. All calculations were performed using the PBE functional[39]

and on-the-fly-generated ultrasoft pseudopotentials, with a cut-off energy of 600 eV. All atomic positions were geometry optimization with the center of mass and unit-cell parameters fixed as their diffraction-determined values, with integrals taken over the Brillouin zone using a Monkhorst–Pack grid with a maximum k-point sample spacing of 0.1 \AA^{-1} and the grid origin at $\mathbf{k} = (\frac{1}{4}, \frac{1}{4}, \frac{1}{4})$ in fractional reciprocal space. Coordinate input files were generated from starting CIF files using CIF2cell[40]. Crystallographically distinct atoms in the output magres files[41] are labelled using the labels in the input CIF files. The NMR parameters were calculated[42] [43] using the same k-point sampling and cut-off energy. The resulting ^{13}C shielding values were converted to chemical shifts using a reference value of 164.4 ppm determined on a subset of ^{13}C resonances that could be unambiguously assigned.

Results and Discussion

Cocrystals of INH were synthesized with CINN and its hydroxy derivatives 4HCA, 3HCA, 2HCA, 24DHCA and 34DHCA. Three cocrystals obtained (INH-4HCA, INH-CINN and INH-34DHCA Form 1) have been reported earlier. The INH-4HCA is previously reported by Ravikumar,[44] cocrystal INH-CINN corresponds to one of the three polymorphic forms reported (Form 4a) by Sarcevic et al.[31][45] and INH-34DHCA Form 1 was previously reported by Swapna et al.[4] All the solid forms were characterized using spectroscopic, thermal and X-ray diffraction techniques. IR studies were also performed, but these were relatively uninformative, and are presented in SI (figure S1).

DSC Results

DSC experiments were carried out to study the thermal behavior of the cocrystals in relation to isoniazid (melting point $172 \text{ }^\circ\text{C}$ [23]). The thermal profile of the cocrystals was distinct (Figure 1), with transition temperatures distinct from those of the individual components, confirming the formation of new solid form. The melting points, calculated from the onset values of the single endothermic transition, for INH-4HCA, INH-3HCA and INH-2HCA were $174 \text{ }^\circ\text{C}$, $165 \text{ }^\circ\text{C}$ and $172 \text{ }^\circ\text{C}$ respectively (reported to the nearest $^\circ\text{C}$). INH-CINN shows melting point at $133 \text{ }^\circ\text{C}$ with a minor thermal event at $125 \text{ }^\circ\text{C}$ (Sarcevic et al.[31] report a melting point of $129\text{--}132 \text{ }^\circ\text{C}$). INH-24DHCA shows two component melt, with onset value of $146 \text{ }^\circ\text{C}$, followed by recrystallization. INH-34DHCA Form 4 has an endothermic peak at $131 \text{ }^\circ\text{C}$, which is likely to be a transformation to Form 1, as the remainder of the curve was a good match to that of Form 1.[4]

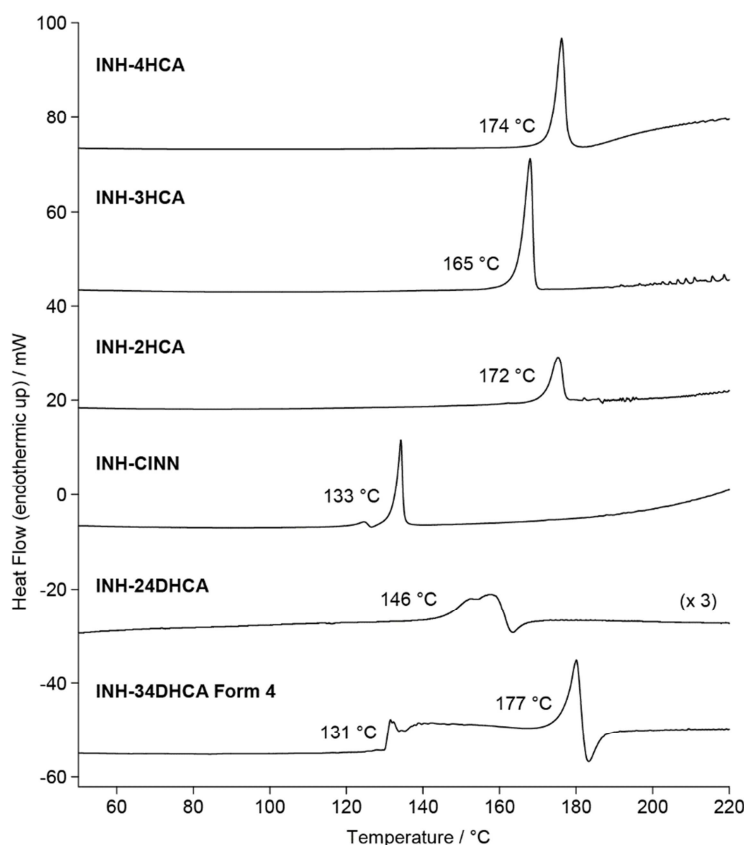


Figure 1: DSC thermogram of the INH cocrystals studied. Figures shown are onset temperatures (rounded to nearest °C).

PXRD Results

In general, the PXRD patterns (Figure 2) are consistent with essentially crystalline products and agree well with PXRD patterns calculated from the single crystal studies. For INH-34DHCA Form 4, the PXRD pattern confirms the formation of essentially crystalline product. However, some extra peaks suggest that this product is not pure. The background intensity in some PXRD patterns (e.g. INH-CINN) suggests the presence of amorphous or poorly crystalline components. For INH-24DHCA, several additional peaks suggest that this product is not pure. For INH-2HCA, there are a few extra peaks that indicates a small amount of unknown impurities, which is consistent with the NMR results discussed below. In the case of INH-CINN, the PXRD pattern is inconsistent with the form (polymorph I) observed from the single-crystal study. Instead, the pattern matches that calculated for polymorph II reported by Sarcevic et al.[31]. The NMR results below confirm that the sample is mostly form II, but with some form I present.

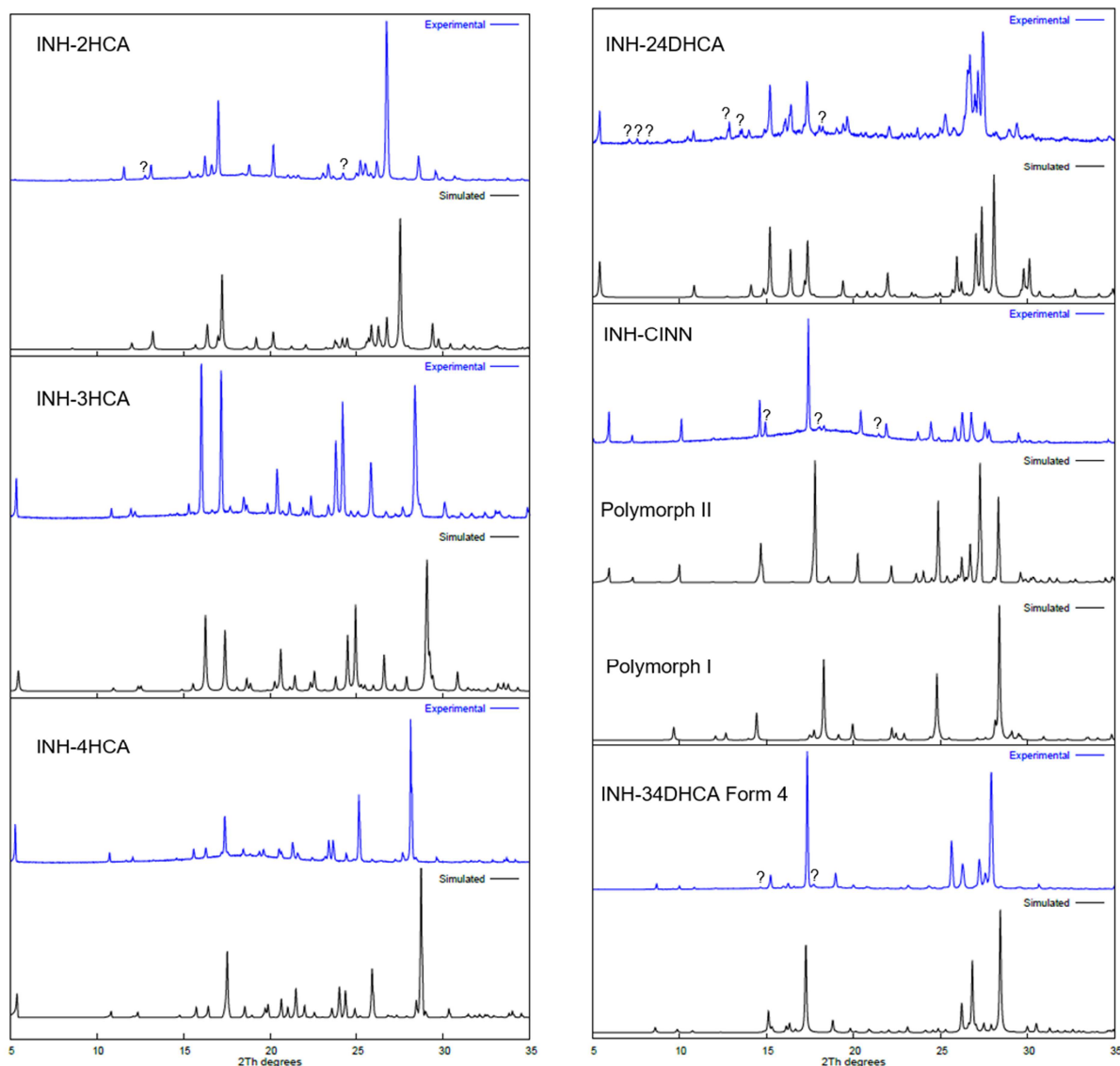


Figure 2. Experimental (blue) and simulated (black) PXRD patterns of the INH cocrystals studied. Calculated patterns were determined from the single crystal XRD structures reported herein, except for INH-CINN polymorph II. Additional peaks corresponding to impurity phases are indicated by question marks.

Single-Crystal XRD Results

The crystal structures of the INH cocrystals were determined by single-crystal X-ray crystallography, as summarized in Table 2. The structures of INH-34DHCA Form 1[4] and INH-CINN Form II[31] have been previously reported, but are re-determined and discussed here for consistency. Figure 3 shows the labelling scheme and hydrogen bonding between the cocrystal components. Detailed views of the crystal packing structures of the cocrystals are shown in SI figures S3 to S9.

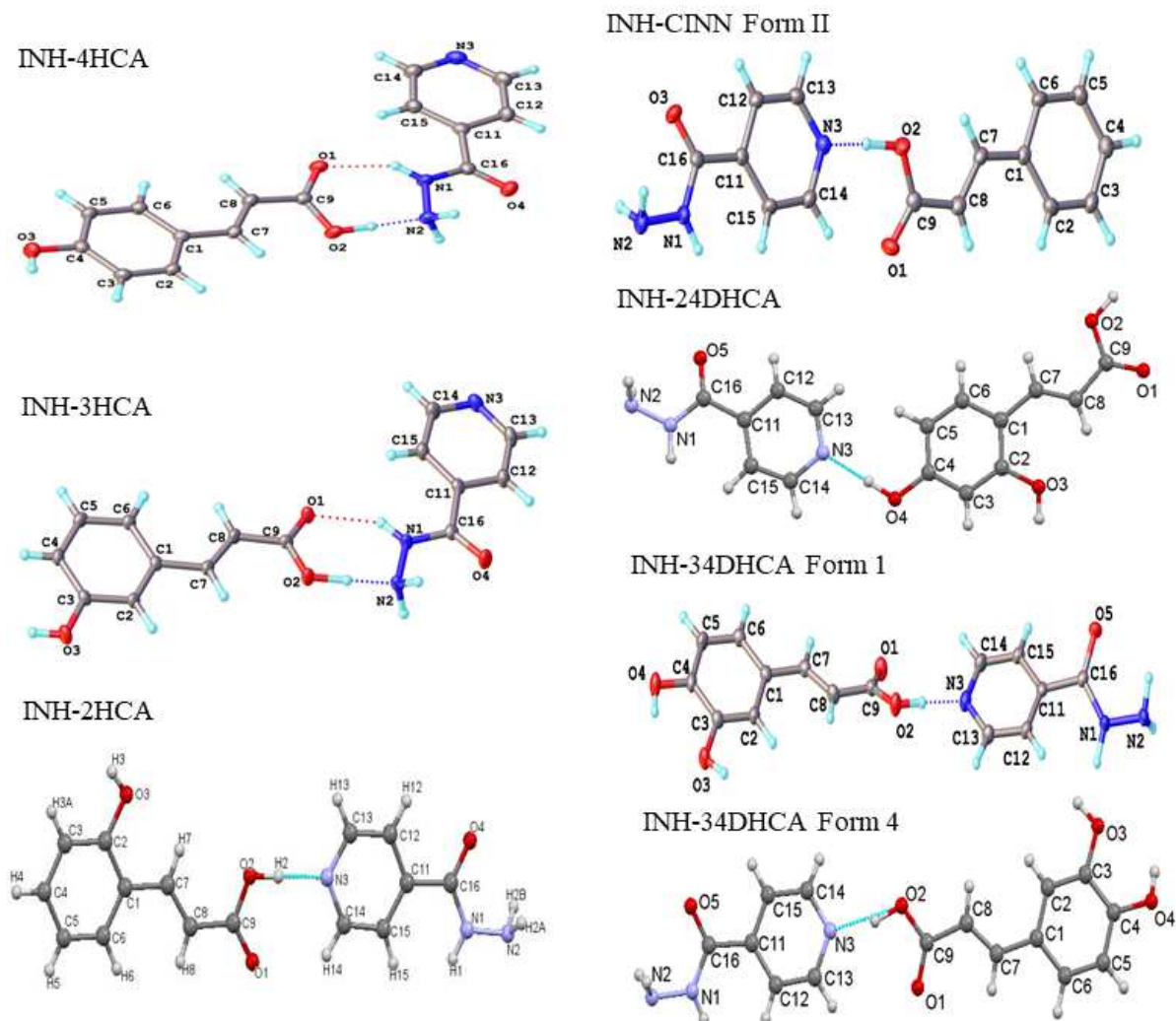
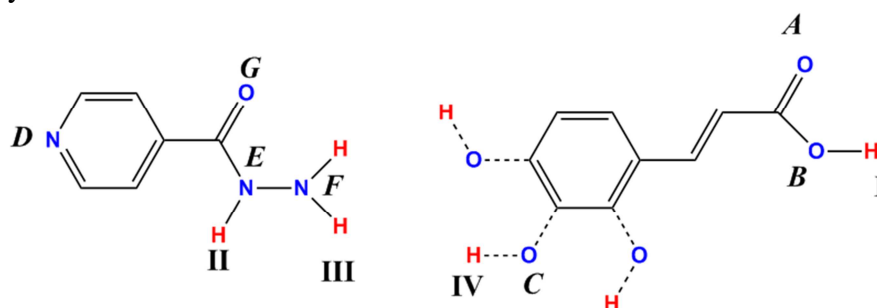


Figure 3: Atomic labelling and key hydrogen bonding between cocrystal components for the different isoniazid cocrystals studied.

The coformer molecules mostly contain four (five for the dihydroxy derivatives, three for CINN) hydrogen atoms capable of forming classical hydrogen bonds and seven (eight for the dihydroxy derivatives, six for CINN) possible acceptors. These sites are represented schematically in Scheme 2.



Scheme 2: Potential hydrogen bond donor and acceptor sites in the INH cocrystals studied. Donor hydrogen sites are labelled with Roman numbers, potential acceptors of hydrogen bonds with capital letters.

Table 1 lists the hydrogen donors and corresponding acceptors found in the studied cocrystals. There are no strong patterns that can be discerned; for any given donor, there are at least two possible acceptors. The variety of hydrogen bonding (HB) arrangements means that analysis of the structures in terms of supramolecular synthons provides little additional insight (see Figure S10 and Table S1 of the SI). Note that some of HBs in Table 1 are quite long (for example, **III-B** in INH-CINN, N...O 3.388 Å) and only their directionality allows them to be called hydrogen bonds. The table also indicates whether or not aromatic $\pi\cdots\pi$ interactions are present. It is notable that these are not always present despite the planarity of both components. Graph-set analysis[46] of hydrogen bond pattern is performed and is shown in Figure S11.

Table 1. Hydrogen bonds in the studied INH cocrystals tabulated by donor atom, with donor-acceptor distances (in Å) shown in parentheses.

Coformer	I	II	III	III	IV^a	IV^a	$\pi\cdots\pi$ ^b
4HCA	<i>F</i> (2.602)	<i>A</i> (2.887)	<i>A</i> (2.989)	<i>B</i> (2.940)	<i>D (p)</i> (2.731)	–	no
3HCA	<i>F</i> (2.739)	<i>A</i> (2.851)	<i>A</i> (2.995)	<i>B</i> (2.938)	<i>D (m)</i> (2.739)	–	no
2HCA	<i>D</i> (2.632)	<i>A</i> (2.890)	<i>B</i> (3.332)	–	<i>G (o)</i> (2.697)	–	yes
CINN	<i>D</i> (2.603)	<i>A</i> (2.972)	<i>A</i> (3.140)	<i>B</i> (3.388)	–	–	yes
24DHCA	<i>F</i> (2.939)	<i>A</i> (3.059)	<i>A</i> (3.475)	<i>B</i> (2.610)	<i>D (p)</i> (2.765)	<i>A (o)</i> (2.707)	yes
34DHCA Form 1	<i>D</i> (2.608)	<i>G</i> (2.793)	<i>A</i> (2.997)	<i>C (p)</i> (3.022)	<i>C (p)</i> (2.823)	<i>F (m)</i> (2.717)	yes
34DHCA Form 4	<i>D</i> (2.592)	<i>A</i> (2.968)	–	<i>C (p)</i> (2.954)	<i>C (p)</i> (2.758)	<i>G (m)</i> (2.689)	yes

^a Position of hydroxyl group(s) shown in parentheses.

^b Two planar 6-membered aromatic fragments were deemed to be participating in the $\pi\cdots\pi$ interaction if the centroid-centroid distance between them was less than 4 Å and the shift was smaller than 3 Å.³¹

In contrast to some previous cocrystals involving INH and carboxylic acids[4], the most common bonding pattern for carboxylic acids, the centrosymmetrical dimer, was not observed in the studied cocrystals. The carboxylic acid hydrogens (**I**) only form hydrogen bonds with nitrogen atoms (*F*, amino- or *D*, pyridino-) and not with carbonyl (*A* or *G*). The secondary amino-hydrogen atom (**II**) is more active than the primary amino hydrogens (**III**) and forms hydrogen bonds with carbonyl oxygens (*A* or *G*). Some potential weaker hydrogen bonds from the NH₂ group are not formed at all. This contradicts the well-known Etter's first rule "All good proton donors and acceptors are used in hydrogen bonding".[47]

In addition to the classical hydrogen bonds the packing motifs are also affected by a number of weaker interactions, such as C–H...O bonds. This makes a simple geometrical synthon approach inadequate to predict the final crystal packing of the studied systems. However, the pair-wise energy-based analysis, which provides an ultimate insight into the crystal packing forces, is out of scope of this study.

Perhaps the most surprising result is the discovery of an additional polymorph of INH-34DHCA. Two crystal structures, plus a third uncharacterized form, have been published to date, which were denoted INH-CFA[4]. Careful examination of the structures reported shows that the previously reported INH-CFA Form 3 has essentially the same lattice parameters as the new INH-34DHCA form but differs in the conformation of 34DHCA (See SI figure S2); its conformation differs by 180° rotation around the Ph–C=C bond (as indicated in Scheme 1). The new form is denoted here as INH-34DHCA Form 4. The different conformations adopted are shown in figure S2 (SI).

Table 2. Structure refinement data for the INH cocrystals studied.

Identification code	INH-4HCA	INH-3HCA	INH-2HCA	INH-CINN	INH-24DHCA	INH-34DHCA Form 1	INH-34DHCA Form 4
Empirical formula	C ₁₅ H ₁₅ N ₃ O ₄	C ₁₅ H ₁₅ N ₃ O ₄	C ₁₅ H ₁₅ N ₃ O ₄	C ₁₅ H ₁₅ N ₃ O ₃	C ₁₅ H ₁₅ N ₃ O ₅	C ₁₅ H ₁₅ N ₃ O ₅	C ₁₅ H ₁₅ N ₃ O ₅
Formula mass / g mol ⁻¹	301.30	301.30	301.30	285.30	317.30	317.30	317.30
Crystal system	monoclinic	monoclinic	monoclinic	triclinic	triclinic	monoclinic	triclinic
Space group	P2 ₁ /n	P2 ₁ /n	P2 ₁ /n	P-1	P-1	P2 ₁ /c	P-1
a / Å	7.4152(3)	7.2704(10)	7.5515(4)	7.4080(12)	6.1347(3)	7.2622(3)	7.173(4)
b / Å	5.70589(16)	5.7811(8)	8.7908(5)	9.4909(15)	7.0980(4)	20.7242(10)	9.505(5)
c / Å	32.6636(10)	32.257(5)	20.7505(12)	10.1371(16)	16.4732(9)	9.6909(4)	10.884(6)
α / °	90	90	90	96.849(6)	85.619(6)	90	109.231(17)
β / °	92.884(3)	91.730(5)	97.614(3)	103.604(6)	82.673(6)	100.998(4)	90.64(2)
γ / °	90	90	90	101.842(6)	78.468(6)	90	93.174(17)
Volume / Å ³	1380.26(8)	1355.2(3)	1365.35(13)	667.39(19)	696.13(7)	1431.73(11)	699.3(7)
Z	4	4	4	2	2	4	2
ρ _{calc} / g cm ⁻³	1.450	1.477	1.466	1.420	1.514	1.472	1.507
μ / mm ⁻¹	0.107	0.109	0.109	0.101	0.116	0.113	0.115
F(000)	632.0	632.0	632.0	300.0	332.0	664.0	332.0
Refl. collected	23361	21214	21314	12030	12496	19007	9065
Independent refl., R _{int}	3673, 0.0401	3276, 0.0825	3802, 0.0549	2912, 0.0994	3182, 0.0873	3793, 0.0819	3387, 0.0456
Data/restraints/parameters	3673/0/219	3276/0/219	3802/0/259	2912/0/250	3182/0/268	3793/0/268	3387/0/268
Goodness-of-fit on F ²	1.026	1.060	1.011	0.951	0.954	1.027	0.974
Final R ₁ indexes [I ≥ 2σ (I)]	0.0413	0.0534	0.0461	0.0588	0.0563	0.0515	0.0440
Final wR ₂ indexes [all data]	0.1054	0.1241	0.1164	0.1326	0.1234	0.1281	0.1063

Solid-State NMR Studies

Solid-state ¹³C NMR was used for initial identification/screening of the bulk sample; successful formation of a cocrystal was clearly indicated by a ¹³C spectrum that was distinct

from the starting materials (see SI figures S12 to S18 for individual comparisons of spectra of starting and final materials). The value of characterizing the bulk sample is highlighted by a number of syntheses in which minority crystals of starting materials were selected for single crystal diffraction, suggesting, incorrectly, that cocrystals had not been formed.

The ^{13}C solid-state NMR spectra of the materials synthesised are shown in figure 4. In most cases the spectra indicate a phase-pure material distinct from the starting materials. Additional peaks corresponding to unreacted cofomer are clearly identified in the case of INH-4HCA, and more tentatively, in the sample of INH-2HCA (see figures S11 and S13 respectively in the supplementary information). This is consistent with the PXRD, Figure 2, which showed an additional crystalline component in the case of INH-2HCA, while the additional peaks in the INH-4HCA NMR spectrum may be associated with the background feature in the powder diffractogram. There is no evidence of significant fractions of amorphous materials, suggesting that the background observed in the PXRD patterns is due to poorly crystalline fractions. The ^{13}C NMR spectra provide a direct, visual means of assessing the formation of a new crystalline form and its phase purity. Spectral overlap means that 2D NMR data would be required to fully assign the spectra. This is not, however, necessary for the spectra to be used as fingerprints of the different solid forms studied, and so is outside the scope of the current publication. There is one interesting correlation between hydrogen bonding patterns and the ^{13}C chemical shifts. Although the carbonyl of the INH hydrazide (acceptor *G* in Table 1) does not strongly participate in hydrogen bonding itself, its shift ranges between 159 to 161 ppm for structures where the acid OH is hydrogen bonded to the NH_2 of hydrazide, but varies between 164 to 172 ppm when the acid OH is hydrogen bonded to the pyridine nitrogen. This presumably reflects the correlations between hydrogen bonding patterns observed in a synthon analysis (Table S1), where different patterns of hydrogen bonding are observed depending on the hydrogen bonding behaviour of the acid OH. Note that calculated ^{15}N shieldings were also able to discriminate between these overall arrangements, with the NH shift of the hydrazide being most distinctive (see figure S20 in SI). Unfortunately, the extremely long ^1H relaxation times of these system precluded obtaining experimental ^{15}N spectra. Figure S19 of the SI shows ^1H spectra obtained under fast magic-angle spinning. These spectra present some unusual features which are still under investigation and so are not discussed further.

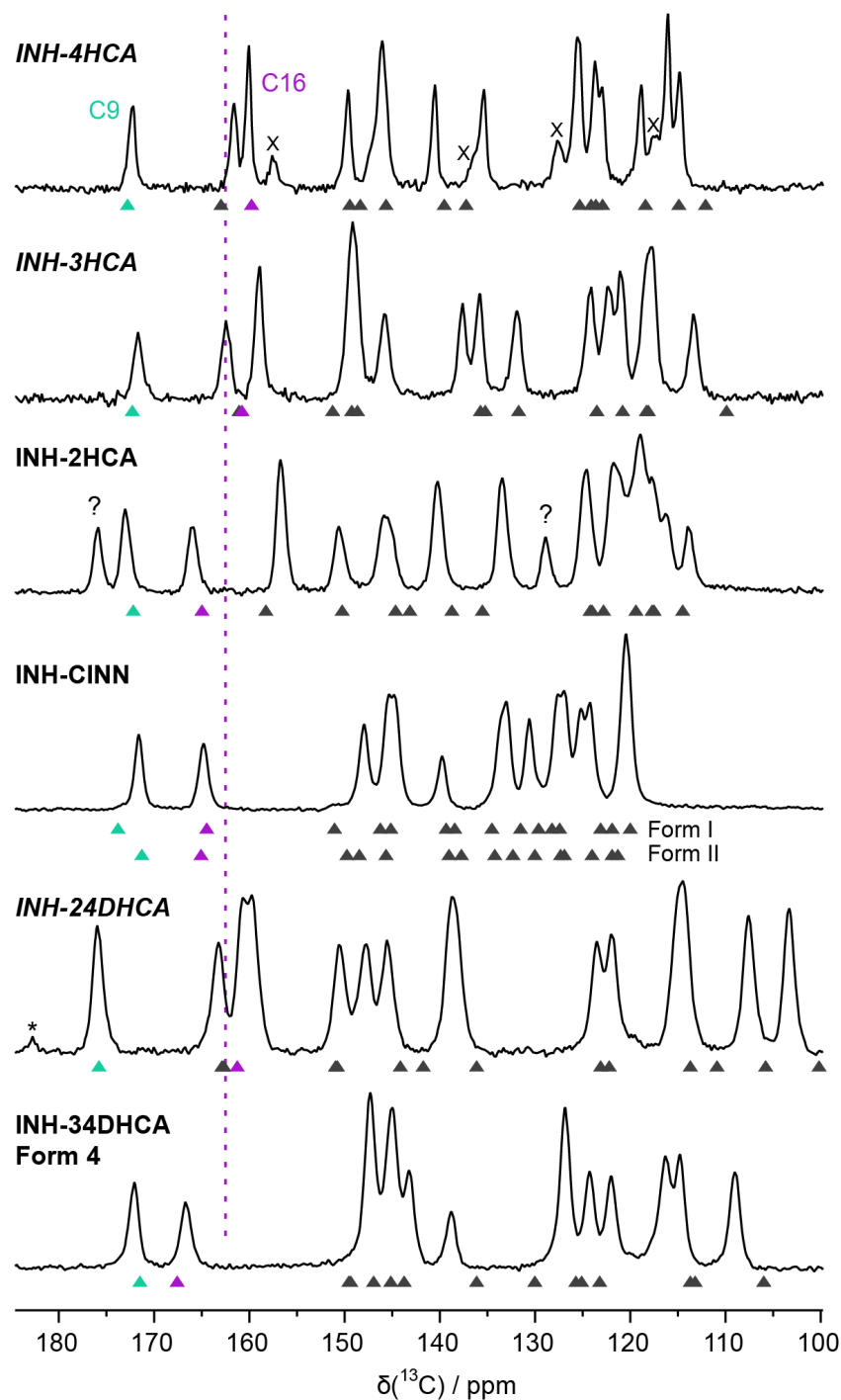


Figure 4: ^{13}C CP/MAS spectra of the isoniazid cocrystals studied. Markers indicate predicted positions of peaks from DFT calculations starting from the single-crystal structures. Two sets of carbonyl resonances are highlighted: the cinnamic acid carbon (C9, turquoise) and the hydrazide carbon (C16, purple); see Fig. 3 for the numbering scheme. The vertical dashed line illustrates the high vs. low frequency separation of the C16 resonance depending on whether the cinnamic acid hydrogen (donor **I**) is hydrogen bonded to acceptor *F* (cocrystal name in italics) or acceptor *D* of Table 1. Asterisks mark spinning sidebands, \times corresponds to an impurity phase of the cofomer. Additional peaks in spectrum of INH-2HCA, probably from the cofomer are indicated with a question mark.

Conclusion

Isoniazid (INH) readily forms cocrystals with hydroxyl derivatives of cinnamic acids due to the complementary nature of the functional groups of INH and the chosen cofomers. The three previously unknown cocrystal forms, plus a new polymorph were characterized by solid-state NMR, DSC, PXRD and their structures were determined by single-crystal XRD. The tendency of 3,4-dihydroxycinnamic acid to form polymorphs when cocrystallized with isoniazid was confirmed by the production of an additional polymorph (Form 4). The new form differs only in the conformation of 3,4-DHCA by 180° rotation around the Ph–C=C bond with all other same parameters. ¹³C solid-state NMR is observed to play a valuable complementary role to PXRD in evaluating phase purity and the extent of cocrystal formation. Individual ¹³C chemical shifts were observed to distinguish between alternative hydrogen bonding arrangements, which may provide valuable constraints in cases where the structure needs to be solved from PXRD data.[48] Synthesized cocrystals might be able to replace INH in the existing FDCs used to treat TB by expected mitigation of degradation of RIF and INH from hydrazone formation by masking the key hydrazide group through cocrystallization. This study also renders an opportunity to combine INH with an antioxidant in a single tablet.

Acknowledgements

We are thankful to HEC Pakistan for providing funding for this project, Dr David Apperley for invaluable assistance with the ¹³C and ¹H NMR experiments, Prof. Ivana Evans for advice on crystallographic aspects, and Mr Douglas Carswell for the DSC experiments.

References

- [1] H. Bhutani, S. Singh, K.C. Jindal, Drug-drug interaction studies on first-line anti-tuberculosis drugs, *Pharm. Dev. Technol.* 10 (2005) 517–524. <https://doi.org/10.1080/10837450500299982>.
- [2] S.A. Carvalho, E.F. da Silva, M.V.N. de Souza, M.C.S. Lourenço, F.R. Vicente, Synthesis and antimycobacterial evaluation of new trans-cinnamic acid hydrazide derivatives, *Bioorganic Med. Chem. Lett.* 18 (2008) 538–541. <https://doi.org/10.1016/j.bmcl.2007.11.091>.
- [3] M.D. Iseman, Tuberculosis therapy: past, present and future, *Eur. Respir. J.* 20 (2002) 87S-94s. <https://doi.org/10.1183/09031936.02.00309102>.
- [4] B. Swapna, D. Maddileti, A. Nangia, Cocrystals of the tuberculosis drug isoniazid: Polymorphism, isostructurality, and stability, *Cryst. Growth Des.* 14 (2014) 5991–6005. <https://doi.org/10.1021/cg501182t>.
- [5] C.J. Shishoo, S.A. Shah, I.S. Rathod, S.S. Savale, M.J. Vora, Impaired bioavailability of rifampicin in presence of isoniazid from fixed dose combination (FDC) formulation, *Int. J. Pharm.* 228 (2001) 53–67. [https://doi.org/10.1016/S0378-5173\(01\)00831-6](https://doi.org/10.1016/S0378-5173(01)00831-6).
- [6] S. Battini, M.K.C. Mannava, A. Nangia, Improved Stability of Tuberculosis Drug Fixed-Dose Combination Using Isoniazid-Caffeic Acid and Vanillic Acid Cocrystal, *J. Pharm. Sci.* 107 (2018) 1667–1679. <https://doi.org/10.1016/j.xphs.2018.02.014>.
- [7] H. Bhutani, S. Singh, K.C. Jindal, A.K. Chakraborti, Mechanistic explanation to the catalysis by pyrazinamide and ethambutol of reaction between rifampicin and isoniazid in anti-TB FDCs, *J. Pharm. Biomed. Anal.* 39 (2005) 892–899. <https://doi.org/10.1016/j.jpba.2005.05.015>.
- [8] H. Bhutani, T.T. Mariappan, S. Singh, An explanation for the physical instability of a marketed fixed dose combination (FDC) formulation containing isoniazid and

- ethambutol and proposed solutions, *Drug Dev. Ind. Pharm.* (2004). <https://doi.org/10.1081/DDC-120039184>.
- [9] M. Singh, P. Sasi, V.H. Gupta, G. Rai, D.N. Amarpurkar, P.P. Wangikar, Protective effect of curcumin, silymarin and N-acetylcysteine on antitubercular drug-induced hepatotoxicity assessed in an in vitro model, *Hum. Exp. Toxicol.* 31 (2012) 788–797. <https://doi.org/10.1177/0960327111433901>.
- [10] L.R.C. De Oliveira, E. Peresi, F.C. Tavares, C.R. Corrêa, D.T. Pierine, S.A. Calvi, DNA damage in peripheral blood mononuclear cells of patients undergoing anti-tuberculosis treatment, *Mutat. Res. - Genet. Toxicol. Environ. Mutagen.* 747 (2012) 82–85. <https://doi.org/10.1016/j.mrgentox.2012.04.003>.
- [11] I. Verma, S.K. Jindal, N.K. Ganguly, Oxidative Stress in Tuberculosis, in: N.K. Ganguly, S.K. Jindal, S. Biswal, P.J. Barnes, R. Pawankar (Eds.), *Stud. Respir. Disord.*, Springer New York, New York, NY, 2014: pp. 101–114. https://doi.org/10.1007/978-1-4939-0497-6_6.
- [12] E. Pontiki, D. Hadjipavlou-Litina, K. Litinas, G. Geromichalos, Novel cinnamic acid derivatives as antioxidant and anticancer agents: Design, synthesis and modeling studies, *Molecules.* 19 (2014) 9655–9674. <https://doi.org/10.3390/molecules19079655>.
- [13] G.R. Silveira, K.A. Campelo, G.R.S. Lima, L.P. Carvalho, S.S. Samarão, O. Vieira-Da-Motta, L. Mathias, C.R.R. Matos, I.J.C. Vieira, E.J.T. de Melo, E.J. Maria, In vitro anti-toxoplasma gondii and antimicrobial activity of amides derived from cinnamic acid, *Molecules.* 23 (2018) 9–11. <https://doi.org/10.3390/molecules23040774>.
- [14] N. Rastogi, K.S. Goh, L. Horgen, W.W. Barrow, Synergistic activities of antituberculous drugs with cerulenin and trans-cinnamic acid against Mycobacterium tuberculosis, *FEMS Immunol. Med. Microbiol.* 21 (1998) 149–157. [https://doi.org/10.1016/S0928-8244\(98\)00044-3](https://doi.org/10.1016/S0928-8244(98)00044-3).
- [15] M. Sova, Antioxidant and Antimicrobial Activities of Cinnamic Acid Derivatives, *Mini Rev Med Chem.* 12 (2012) 749–767. <https://doi.org/10.2174/138955712801264792>.
- [16] M. Oruganti, P. Khade, U.K. Das, D.R. Trivedi, The hierarchies of hydrogen bonds in salts/cocrystals of isoniazid and its Schiff base - A case study, *RSC Adv.* 6 (2016) 15868–15876. <https://doi.org/10.1039/c5ra14951g>.
- [17] Y.M. Chen, N. Rodríguez-Hornedo, Cocrystals Mitigate Negative Effects of High pH on Solubility and Dissolution of a Basic Drug, *Cryst. Growth Des.* 18 (2018) 1358–1366. <https://doi.org/10.1021/acs.cgd.7b01206>.
- [18] J.M. Lehn, Toward self-organization and complex matter, *Science* (80-.). 295 (2002) 2400–2403. <https://doi.org/10.1126/science.1071063>.
- [19] M.C. Etter, C.G. Choo, S.M. Reutzel, Self-Organization of Adenine and Thymine in the Solid State, *J. Am. Chem. Soc.* (1993). <https://doi.org/10.1021/ja00063a089>.
- [20] N. Shan, M.J. Zaworotko, The role of cocrystals in pharmaceutical science, *Drug Discov. Today.* 13 (2008) 440–446. <https://doi.org/10.1016/j.drudis.2008.03.004>.
- [21] N. Schultheiss, A. Newman, Pharmaceutical cocrystals and their physicochemical properties, *Cryst. Growth Des.* (2009). <https://doi.org/10.1021/cg900129f>.
- [22] D. Douroumis, A. Nokhodchi, Preface: Engineering of pharmaceutical cocrystals, salts and polymorphs: Advances and Challenges, *Adv. Drug Deliv. Rev.* (2017). <https://doi.org/10.1016/j.addr.2017.10.002>.
- [23] S.M.A. Mashhadi, U. Yunus, M.H. Bhatti, I. Ahmed, M.N. Tahir, Synthesis, characterization, solubility and stability studies of hydrate cocrystal of antitubercular Isoniazid with antioxidant and anti-bacterial Protocatechuic acid, *J. Mol. Struct.* 1117 (2016) 17–21. <https://doi.org/10.1016/j.molstruc.2016.03.057>.
- [24] A. Karagianni, M. Malamataris, K. Kachrimanis, Pharmaceutical cocrystals: New solid phase modification approaches for the formulation of APIs, *Pharmaceutics.* 10 (2018)

- 1–30. <https://doi.org/10.3390/pharmaceutics10010018>.
- [25] N.K. Duggirala, M.L. Perry, Ö. Almarsson, M.J. Zaworotko, Pharmaceutical cocrystals: Along the path to improved medicines, *Chem. Commun.* 52 (2016) 640–655. <https://doi.org/10.1039/c5cc08216a>.
- [26] M. Karimi-Jafari, L. Padrela, G.M. Walker, D.M. Croker, Creating cocrystals: A review of pharmaceutical cocrystal preparation routes and applications, *Cryst. Growth Des.* 18 (2018) 6370–6387. <https://doi.org/10.1021/acs.cgd.8b00933>.
- [27] M. Žegarac, E. Lekšić, P. Šket, J. Plavec, M. Devčić Bogdanović, D.K. Bučar, M. Dumić, E. Meštrović, A sildenafil cocrystal based on acetylsalicylic acid exhibits an enhanced intrinsic dissolution rate, *CrystEngComm.* (2014). <https://doi.org/10.1039/c3ce42013b>.
- [28] G.R. Desiraju, Supramolecular Synthons in Crystal Engineering—A New Organic Synthesis, *Angew. Chemie Int. Ed. English.* 34 (1995) 2311–2327. <https://doi.org/10.1002/anie.199523111>.
- [29] D.J. Berry, J.W. Steed, Pharmaceutical cocrystals, salts and multicomponent systems; intermolecular interactions and property based design, *Adv. Drug Deliv. Rev.* 117 (2017) 3–24. <https://doi.org/10.1016/j.addr.2017.03.003>.
- [30] S.M.A. Mashhadi, U. Yunus, M.H. Bhatti, M.N. Tahir, Isoniazid cocrystals with antioxidant hydroxy benzoic acids, *J. Mol. Struct.* 1076 (2014) 446–452. <https://doi.org/10.1016/j.molstruc.2014.07.070>.
- [31] I. Sarcevic, L. Orola, M. V. Veidis, A. Podjava, S. Belyakov, Crystal and molecular structure and stability of isoniazid cocrystals with selected carboxylic acids, *Cryst. Growth Des.* 13 (2013) 1082–1090. <https://doi.org/10.1021/cg301356h>.
- [32] P. Hodgkinson, NMR Crystallography of Molecular Organics, *Prog. Nucl. Magn. Reson. Spectrosc.* (2020). <https://doi.org/10.1016/J.PNMRS.2020.03.001>.
- [33] M.R. Chierotti, R. Gobetto, Solid-State NMR Studies on Supramolecular Chemistry, in: *Supramol. Chem.*, John Wiley & Sons, Ltd, 2012. <https://doi.org/10.1002/9780470661345.smc026>.
- [34] F.G. Vogt, J.S. Clawson, M. Strohmeier, A.J. Edwards, T.N. Pham, S.A. Watson, Solid-State NMR Analysis of Organic Cocrystals and Complexes, *Cryst. Growth Des.* 9 (2008) 921–937. <https://doi.org/10.1021/cg8007014>.
- [35] Ł. Szeleszczuk, D.M.I. Pisklak, M. Zielińska-Pisklak, I. Wawer, Effects of structural differences on the NMR chemical shifts in cinnamic acid derivatives: Comparison of GIAO and GIPAW calculations, *Chem. Phys. Lett.* 653 (2016) 35–41. <https://doi.org/10.1016/j.cplett.2016.04.075>.
- [36] O. V. Dolomanov, L.J. Bourhis, R.J. Gildea, J.A.K. Howard, H. Puschmann, OLEX2: A complete structure solution, refinement and analysis program, *J. Appl. Crystallogr.* 42 (2009) 339–341. <https://doi.org/10.1107/S0021889808042726>.
- [37] G.M. Sheldrick, Crystal structure refinement with SHELXL, *Acta Crystallogr. Sect. C Struct. Chem.* 71 (2015) 3–8. <https://doi.org/10.1107/S2053229614024218>.
- [38] S.J. Clark, M.D. Segall, C.J. Pickard, P.J. Hasnip, M.I.J. Probert, K. Refson, M.C. Payne, First principles methods using CASTEP, *Zeitschrift Fur Krist.* 220 (2005) 567–570. <https://doi.org/10.1524/zkri.220.5.567.65075>.
- [39] J.P. Perdew, K. Burke, M. Ernzerhof, Generalized gradient approximation made simple, *Phys. Rev. Lett.* 77 (1996) 3865–3868. <https://doi.org/10.1103/PhysRevLett.77.3865>.
- [40] T. Björkman, CIF2Cell: Generating geometries for electronic structure programs, *Comput. Phys. Commun.* 182 (2011) 1183–1186. <https://doi.org/10.1016/j.cpc.2011.01.013>.
- [41] S. Sturniolo, T.F.G. Green, R.M. Hanson, M. Zilka, K. Refson, P. Hodgkinson, S.P. Brown, J.R. Yates, Visualization and processing of computed solid-state NMR

- parameters: MagresView and MagresPython, *Solid State Nucl. Magn. Reson.* 78 (2016) 64–70. <https://doi.org/10.1016/j.ssnmr.2016.05.004>.
- [42] C.J. Pickard, F. Mauri, All-electron magnetic response with pseudopotentials: NMR chemical shifts, *Phys. Rev. B.* 63 (2001). <https://doi.org/10.1103/physrevb.63.245101>.
- [43] J.R. Yates, C.J. Pickard, F. Mauri, Calculation of NMR chemical shifts for extended systems using ultrasoft pseudopotentials, *Phys. Rev. B - Condens. Matter Mater. Phys.* 76 (2007). <https://doi.org/10.1103/PhysRevB.76.024401>.
- [44] N. Ravikumar, G. Gaddamanugu, K. Anand Solomon, Structural, spectroscopic (FT-IR, FT-Raman) and theoretical studies of the 1:1 cocrystal of isoniazid with p-coumaric acid, *J. Mol. Struct.* (2013). <https://doi.org/10.1016/j.molstruc.2012.10.029>.
- [45] I. Sarcevic, L. Orola, M. V. Veidis, S. Belyakov, Cinnamic acid hydrogen bonds to isoniazid and N²-(propan-2-ylidene) isonicotinohydrazide, an in situ reaction product of isoniazid and acetone, *Acta Crystallogr. Sect. C Struct. Chem.* 70 (2014) 392–395. <https://doi.org/10.1107/S2053229614003684>.
- [46] M.C. Etter, J.C. MacDonald, J. Bernstein, Graph set analysis of hydrogen bond patterns in organic crystals, *Acta Crystallogr. Sect. B.* (1990). <https://doi.org/10.1107/S0108768189012929>.
- [47] M.C. Etter, Encoding and Decoding Hydrogen-Bond Patterns of Organic Compounds, *Acc. Chem. Res.* 23 (1990) 120–126. <https://doi.org/10.1021/ar00172a005>.
- [48] C.E. Hughes, G.N.M. Reddy, S. Masiero, S.P. Brown, P.A. Williams, K.D.M. Harris, Determination of a complex crystal structure in the absence of single crystals: Analysis of powder X-ray diffraction data, guided by solid-state NMR and periodic DFT calculations, reveals a new 2'-deoxyguanosine structural motif, *Chem. Sci.* 8 (2017) 3971–3979. <https://doi.org/10.1039/c7sc00587c>.

Highlights

- Three novel cocrystal and a new polymorph cocrystal of isoniazid are synthesized
- All structures are characterized by IR, DSC, PXRD, ^{13}C Solid-State NMR and Single crystal XRD techniques
- Three previously known cocrystals of isoniazid are synthesized and characterised
- ^{13}C solid-state NMR is observed to play a valuable complementary role to PXRD in evaluating phase purity and the extent of cocrystal formation
- ^{13}C chemical shifts are observed to distinguish between alternative hydrogen bonding arrangements

Declaration of interests

The authors declare that they have no known competing financial interests or personal relationships that could have appeared to influence the work reported in this paper.

The authors declare the following financial interests/personal relationships which may be considered as potential competing interests:

Journal Pre-proof